The Egyptian Journal of Radiology and Nuclear Medicine (2014) **45**, 535–542

Egyptian Society of Radiology and Nuclear Medicine

The Egyptian Journal of Radiology and Nuclear Medicine

www.elsevier.com/locate/ejrnm
www.sciencedirect.com

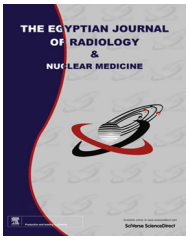

ORIGINAL ARTICLE

Diffusion-weighted MR imaging and ADC measurement in normal prostate, benign prostatic hyperplasia and prostate carcinoma

Sally Emad-Eldin [a,*], **Manal Halim** [a], **Lamiaa I.A. Metwally** [a], **Rania Mahmoud Abdel-Aziz** [b]

[a] *Diagnostic and Intervention Radiology Department, Cairo University Hospitals, Kasr Al-Ainy, Cairo, Egypt*
[b] *Radiotherapy Department, National Cancer Institute, Cairo University, Cairo, Egypt*

Received 19 February 2014; accepted 25 February 2014
Available online 28 March 2014

KEYWORDS

MRI;
Diffusion;
ADC;
BPH;
Prostate carcinoma

Abstract *Purpose:* Our aim was to investigate the diffusion-weighted Imaging (DWI) appearance and apparent diffusion coefficient (ADC) values of normal prostatic gland, prostate carcinoma (PCa) and benign prostate hyperplasia (BPH) and to determine the utility of DWI in their characterization.

Materials and methods: During a period of 16 months, 40 consecutive patients, with elevated PSA level and 12 healthy volunteers with no clinical symptoms or history of prostate disease were prospectively evaluated with DWI of the prostate. MRI was performed using a 1.5T MR scanner equipped with a pelvic phased array coil. For anatomical imaging, T2W FSE in the three orthogonal planes, and T1WI in axial plane were obtained. DWI with b values of 0, 300, 500 and 800 s/mm^2 were performed in axial plane. The results were confirmed by TRUS-guided biopsy or prostatectomy.

Results: Patients ranged in age from 45 to 85 years (mean 66.6 ± 7.9 year). Twenty patients were confirmed to have BPH, whereas 20 patients had PCa. The mean and SD of ADC values for the peripheral zone (PZ), central gland (CG), BPH nodules and PCa were 1.839 ± 0.233, 1.469 ± 0.239, 1.359 ± 0.201 and 0.87 ± 0.13 respectively. The mean ADC value of PCa was significantly lower than that of CG, PZ, and BPH nodule, with p value < 0.05.

* Corresponding author. Address: Diagnostic and Intervention Radiology department, Cairo University Hospitals, Kasr Al-Ainy, EL-Manial, 11956 Cairo, Egypt. Tel.: +20 0106 1616935; fax: +20 02 23687673.
E-mail address: sallyemad@hotmail.com (S. Emad-Eldin).

Peer review under responsibility of Egyptian Society of Radiology and Nuclear Medicine.

ELSEVIER Production and hosting by Elsevier

http://dx.doi.org/10.1016/j.ejrnm.2014.02.017

Conclusion: DW MR imaging characteristics and ADC values can differentiate PCa and BPH. DWI with ADC may be used as a complementary method to conventional MRI in diagnosis of PCa and BPH.

1. Introduction

Benign prostatic hyperplasia (BPH) and prostate carcinoma (PCa) are the most common diseases of the prostate. During the past several years, their morbidities have increased sharply all over the world. Therefore, early diagnosis and differential diagnosis of prostatic diseases have caught the attention of physicians. Many imaging methods have been widely used in the diagnosis of prostatic diseases (1).

MRI has been considered as an excellent technique for detection of prostatic carcinoma (2). High-spatial-resolution T2-weighted rapid acquisition with a small field of view, performed with endorectal and/or external body phased-array coils, is generally used to depict prostate anatomy. On T2-weighted images, prostate cancer appears as an area of low signal intensity within the high signal intensity of a normal peripheral zone (3).

However, anatomic T2-weighted MR imaging has limited diagnostic value in discriminating prostate cancer from benign prostate tissue, as focal areas of low signal intensity in the peripheral zone do not always represent cancer (4).

Benign abnormalities such as chronic prostatitis, atrophy, scars, post-irradiation or hormonal treatment effects, hyperplasia, and post biopsy hemorrhage may mimic tumor tissue (5). Furthermore, 30% of tumours that occur in the central gland cannot be detected on T2 weighted imaging because it is not possible to differentiate them from the low signal-intensity benign nodules of prostatic hyperplasia (6).

Of all functional MR imaging techniques diffusion-weighted imaging (DWI) is the most practical and simple in its use (3). It has the advantages of not requiring IV contrast material and of being simple to process. Moreover, DWI requires less time to acquire than proton MR spectroscopy and less technologist training to perform (7). However it has the disadvantages of being susceptible to motion and to magnetic field inhomogeneities (3).

DW imaging has been shown to aid in distinguishing between malignant and benign prostate tissue based on relatively lower apparent diffusion coefficients (ADCs) of cancer tissue (5,8). The extensive branching ductal structure of the normal prostate compared with the highly restricted intracellular and interstitial spaces encountered in prostate cancers produces a substantial differential in apparent diffusion coefficient (ADC), and thus the potential for high image contrast (6).

Our aim was investigating the DWI appearance and ADC values of normal prostatic gland, prostate carcinoma (PCa) and benign prostate hyperplasia (BPH) and to determine the utility of DWI in their characterization.

2. Materials and methods

2.1. Patients

During a period of 16 months duration from June 2012 to September 2013, 40 consecutive patients, with elevated PSA level and 12 healthy volunteers with no clinical symptoms or history of prostate disease were prospectively evaluated with MRI diffusion of the prostate. This study was performed after the approval of the scientific and ethics committee of the hospital. Informed consents were obtained from patients and volunteers.

The patients presented with dysuria, frequent micturition, urgency, weak stream and retention of urine or gross hematuria. TRUS was done to all patients prior to MRI examination, whereas TRUS-guided biopsy was done to 10 patients before MRI examination. The rest of the patients underwent MRI examination followed by TRUS guided biopsy. The time interval ranges between MRI and biopsy from 20 days to 1 month. No patient had a history of pelvic irradiation, thermal, hormonal therapy to the prostate or chemotherapy.

The results of MRI were confirmed by TRUS-guided biopsy or prostatectomy. Ten BPH patients were subjected to trans-urethral resection of the prostate (TURP) whereas 7 underwent open prostatectomies, 3 received medical treatment. Among the 20 prostate cancer patients, 13 patients underwent radical prostatectomy, 1 patient underwent both radical prostatectomy and orchiectomy while 2 patients received external beam radiation therapy following orchiectomy, and 4 patients received radiation therapy.

2.2. MR imaging

The MRI examinations were performed using a 1.5-Tesla MR scanner (Gyroscan Intera, Philips medical systems, Netherlands). MRI examinations were obtained with body coil in supine position. For anatomical imaging of the prostate T2 weighted fast spin-echo (FSE) in the three orthogonal planes, axial, sagittal and coronal planes were obtained with the following parameters:[TR/effective TE] 2000/90 ms, echo train length 16, number of signal average (NSA) 2. FOV 14 cm^2, acquisition matrix 256×512, number of contiguous slices 20, slice thickness 3 mm and interslice gap 0.5 mm.

T1-weighted turbo spin-echo (TSE) in axial plane was obtained with the following parameters: TR/TE 400/10 ms, NSA 2, FOV 14 cm^2, matrix 256×150, number of contiguous slices 20, slice thickness 3 mm; interslice gap 0.5 mm; acquisition time 4 min.

Echo-planar diffusion-weighted sequences with b values of 0, 500 and 800 s/mm^2 were performed in the axial plane with orientation and location identical to those performed for the axial T2-weighted anatomic images. Spin-echo echo-planar imaging (EPI) sequence with a pair of rectangular gradient pulses along with three orthogonal axes was obtained with the following parameters: TR/TE:3600/110 ms, echo train length 16, number of signal average (NSA) 2, FOV 14 cm^2, acquisition matrix 256×512, number of contiguous slices 20, slice thickness 3 mm and inter-slice gap 0.5 mm.

Table 1 Demographic data of the patients.

	Age	PSA level (ng/mL)
BPH	66.5 years ± 8.6 (48–80)	13.53
PCa	67.1 years ± 6.9 (55–85)	60.41

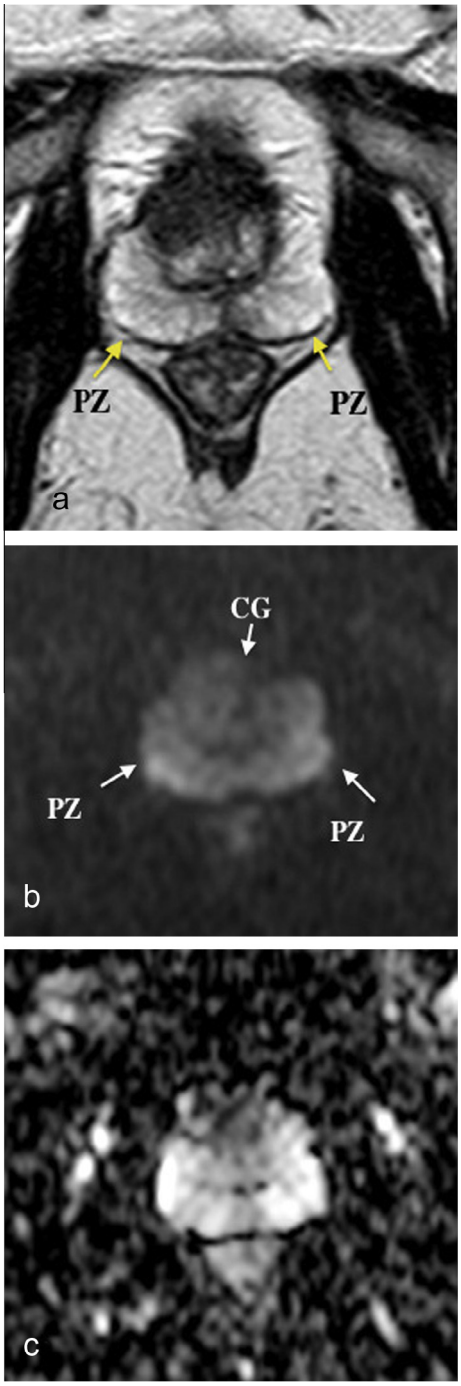

Fig. 1 Normal prostate. (a) Axial T2 WI of prostate gland showing normal prostate parenchyma with hyper-intense PZ. (b) Diffusion WI showing the normal homogenous signal of the CG and PZ. (c) ADC map: The calculated mean ADC value of the PZ is 1.917×10^{-3} mm^2/s. The calculated mean ADC value of the CG is 1.304×10^{-3} mm^2/s.

2.3. Analysis of MR images and ADC measurement

The locations, contour and edges of the lesions on T2WI were evaluated. Analysis of diffusion images was performed qualitatively by means of visual assessment of signal intensity on images acquired at high b values and their corresponding ADC maps and quantitatively by means of ADC measurements.

Prostate cancer was defined as a lesion with focal or diffuse hypo-intensity on T2WI with corresponding hyperintensity on DWI and low value on ADC map compared to the rest of the gland. BPH was defined as central gland nodule with heterogeneous high or low signal intensity.

In cases of prostate cancer, invasion of the neurovascular bundles, breaching of the prostatic capsule, involvement of the seminal vesicles were evaluated, together with the presence of metastatic pelvic lymph nodes and bone deposits of the pelvic bones.

2.4. ADC calculation

DWI datasets were transferred to an independent workstation (Philips MR extended workspace, software version 2009). ADC maps were calculated automatically with the MRI system and ADC values were expressed in square millimeters per second.

The DWI images, including the images obtained with b values of 0, 500, and 800 s/mm^2, were reviewed together. ADCs were measured from each lesion for b 800 s/mm2 by using ROIs (regions of interest). The size of ROIs was chosen to be as large as possible and with minimal contamination from normal tissue. At least three measurements were performed and the least value was recorded. Circular ROIs were placed in the normal central and peripheral zones of the normal individuals.

The ADC values of BPH and PCa lesions were compared with the histological results of prostatectomy and biopsy specimen.

We also compared the performance of T2 weighted MRI alone versus T2 combined with DWI in localization of PCa.

3. Statistical analysis

Statistical analysis was performed with SPSS (Statistical Package for the Social Sciences) V21. ADC values were defined as mean ± standard deviation. An independent sample *t*-test was conducted to examine whether there was a significant difference between ADC value of normal peripheral zone (PZ), normal central gland (CG), BPH nodules and prostate carcinoma. The differences in the ADC values were considered to be statistically significant when the p value was < 0.05.

4. Results

The 40 patients enrolled in this study were ranging in age from 45 to 85 years (mean age 66.6 ± 7.9 year). Twenty patients were confirmed to have BPH, whereas 20 patients had prostate cancer. Demographic data of the patients are demonstrated in Table 1.

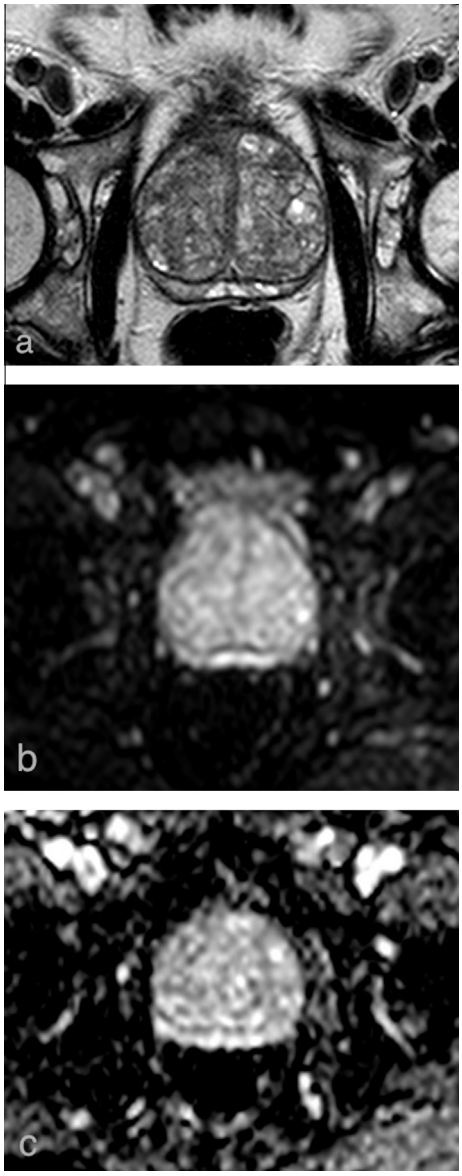

Fig. 2 BPH in 68-year old male, PSA level 12.2 ng/mL. (a) Axial T2 WI of the prostate showing enlarged heterogeneous CG with compressed PZ. (b) Diffusion WI showing no areas of diffusion restriction. (c) ADC map showing non-uniform signal intensity of the CG, the calculated ADC value of the CG is 1.12×10^{-3} mm^2/s, the calculated ADC value of the PZ is 1.35×10^{-3} mm^2/s.

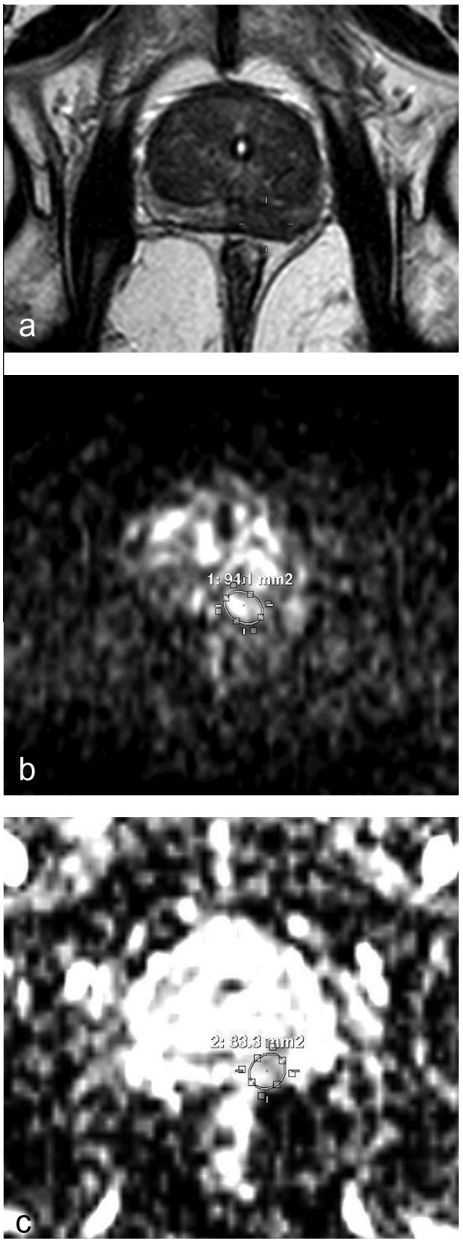

Fig. 3 PCa in 70-year old male, PSA level 30.7 ng/mL, Gleason score 2 + 3. (a) Axial T2 WI of the prostate showing small hypointense lesion in the left side of the PZ. (b and c) Diffusion WI and ADC map showing restricted diffusion of the lesion, with the ADC value is 0.98×10^{-3} mm^2/s.

4.1. ADC values

The CG and PZ of normal prostate were easily discriminated on diffusion and ADC images (Fig. 1). The signal intensity of BPH nodule was non-homogeneous and lower than that of PZ on ADC map (Fig. 2). PCa showed high signal intensity on DWI and low signal intensity on ADC map (Figs. 3 and 4).

The ADC value was obtained from all volunteers and patients. The mean and standard deviation (SD) ADC values for the CG, normal PZ, BPH nodules and prostate carcinomas are presented in Table 2 for volunteers and patients.

The mean ADC value of prostate carcinoma was significantly lower than that of normal CG, PZ, and BPH nodule (ρ value < 0.05). The PZ tissue had a significantly higher ADC value than CG ($p < 0.05$). The ADC value of BPH lesions was significantly lower than that of CG ($p < 0.05$).

For localization of prostate cancers, the accuracy, sensitivity and specificity for combined T2 and diffusion were 90%,

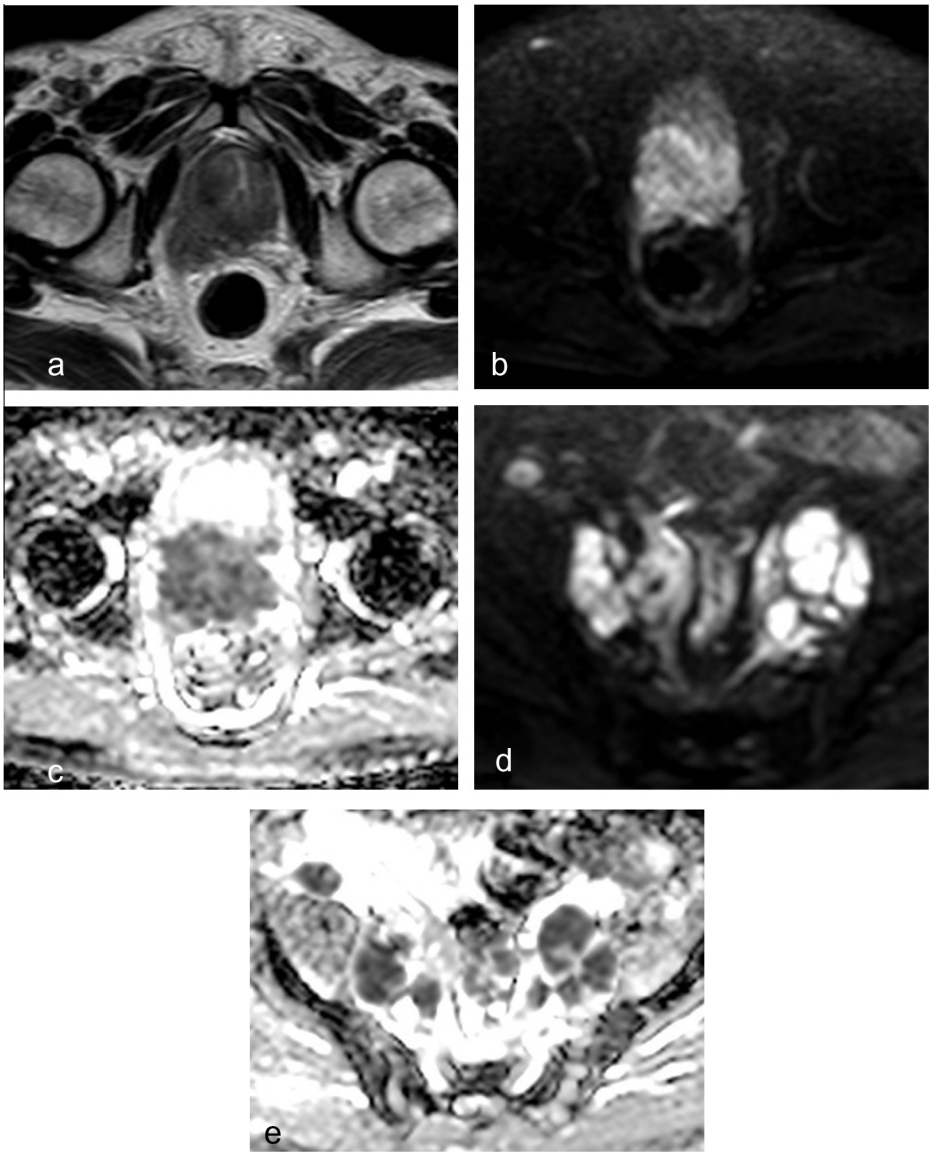

Fig. 4 PCa in 65-year old male, with PSA level 53.9 ng/mL, Gleason score 4 + 3. (a) Axial T2 WI of the prostate showing large hypointense lesion, extending beyond the capsule on the right side, with involvement of the right NVB. (b and c) Diffusion WI and ADC map showing restricted diffusion of the lesion. The ADC value is 0.76×10^{-3} mm^2/s. (d and e) Diffusion WI and ADC map showing restricted diffusion of the metastatic lymph nodes. The ADC value is 0.72×10^{-3} mm^2/s.

Table 2 Mean ADC values (mean ± SD) with *b* value of 800 s/mm^2 for normal peripheral zone (PZ), normal central gland (CG), BPH nodule and prostate carcinoma.

Tissue	Normal Pz	Normal CG	PCa	BPH
ADC ($\times 10^3$ mm^2)	1.839 ± 0.233 (1.5–2.2)	1.469 ± 0.239 (1.3–1.8)	0.87 ± 0.13 (0.6–1.17)	1.359 ± 0.201 (0.8–1.58)
N	12	12	20	20

N: number. SD: standard deviation.

85% and 95% respectively compared to 77.5%, 65% and 90% when using T2 alone.

The (TNM) staging of the primary tumor ranged from T1 to T4, with 2 patients staged as T1, 8 patients as T2, 7 patients as T3 whereas the other 3 patients as T4 (Table 3). Six patients showed nodal metastasis (N1). Six patients showed bony metastasis (M1) in the pelvis which were further confirmed by bone scan.

Table 3 Pathologic characteristics of patients with prostate carcinomas.

T stage	No.
T1	2
T2	8
T3a	3
T3b	4
T4	3

5. Discussion

DWI appears to hold promise as a non-invasive imaging modality in the detection of early microstructural and functional changes of different organs (9). It depicts differences in molecular diffusion caused by the random and microscopic motion of molecules, which is known as Brownian motion (11). In tumors, the motion of water is restricted, due to their higher cellular density and increased nucleocytoplasmic ratio, and it can be depicted on ADC maps, permitting a quantitative evaluation (9).

DW-MRI is feasible on the prostate and the calculation of the ADC values is relatively straightforward. In the prostate tissue, the predominant contribution of the extracellular component is from tubular structures and their fluid content, whereas the intracellular component is determined by the epithelial and stromal cell (9).

In most cases, the PZ can be easily discriminated from the CG, because it displays relatively higher ADC values compared with the PZ (12,13). The CG consists of more compact smooth muscle cells and sparser glandular elements than the PZ, leading to a lower extracellular-to-intracellular fluid ratio and to lower ADC values (14,15).

To optimize the ability of DW imaging to allow characterization of the diffusion properties of tissue, imaging parameters should be optimized according to the imaging unit and magnetic field strength used. Selection of the correct *b* value is particularly important for prostate tissue with a prolonged T2 relaxation time. Use of high *b* values increases diffusion sensitivity by diminishing the hyperintensity of tissues with long T2 relaxation times (thus avoiding T2 shine-through). In general, a high *b* value (>700 s/mm^2 at 1.5 T and >1000 s/mm^2 at 3 T) is recommended for prostate diffusion-weighted imaging (16).

This study was conducted with b value (300, 500 and 800 s/mm^2). The high b values were used to obtain good quality images. An image of low *b*-value (0–300 s/mm^2) has higher SNR, less distortion, but less diffusion weighting. Conversely, high *b*-factor (800 s/mm^2) images have more diffusion weighting but suffer from low signal-to-noise ratio and severe image distortion. Similar *b* values were used in the previous reports of Ren et al. (2) and Yoshimitsu et al. (17).

Diffusion-weighted imaging and ADC have become powerful indicators for characterization of prostatic tissue, particularly in differentiation between benign and malignant lesions (18). Prostate carcinoma is histologically characterized by a higher cellular density than normal prostate tissue, with replacement of the normal glandular tissue; thus, it is expected to show a more impeded diffusion of water molecules, compared with normal prostatic gland (9).

In this study we have found ADC values of the normal PZ, CG, BPH and PCa similar to those reported in the literature. The mean ADC value for normal PZ and CG was $1.839 \pm 0.233 \times 10^{-3}$ mm^2/s, and $1.469 \pm 0.2391 \times 10^{-3}$ mm^2/s respectively. This was in line with the study performed by Tamada et al. (13) who have reported that the mean ADC value of the normal PZ was $1.8 \pm 0.27 \times 10^{-3}$ mm^2/s, normal CG was $1.34 \pm 0.14 \times 10^{-3}$. Ren et al. (2) have also reported that mean ADC values of normal PZ and CG were $1.829 \pm 0.071 \times 10^{-3}$ and $1.352 \pm 0.052 \times 10^{-3}$ mm^2/s respectively (2). Liu et al. reported ADC values of normal PZ and CG were $1.69 \pm 0.28 \times 10^{-3}$, $1.36 \pm 0.12 \times 10^{-3}$ mm^2/s respectively (19).

The mean ADC value of benign prostatic hyperplasia was $1.359 \pm 0.201 \times 10^{-3}$ mm^2/s. This result was in line with that of Lu et al. who reported a mean ADC value for 28 cases of BPH $1.21 \pm 0.21 \times 10^{-3}$ mm^2/s. However this was slightly lower than the value previously reported by Ren et al. (2) for 29 cases of BPH $1.576 \pm 0.099 \times 10^{-3}$ mm^2/s.

The ADC value of BPH was significantly lower than that of normal CG. This was in agreement with the previous results of Liu et al. (19). This can be due to CG tissue in patients with BPH may contain more stroma tissue and concomitantly less glandular components than healthy CG tissue (20).

The mean ADC value for prostatic carcinoma was $0.87 \pm 0.13 \times 10^{-3}$ mm^2/s. This was in agreement with previous results of Ren et al. who reported that a mean ADC value for 21 patients of prostatic carcinoma was $0.934 \pm 0.166 \times 10^{-3}$ mm^2/s (2). In another study Tanimoto A et al. have reported that mean ADC value of PCa was $0.93 \pm 0.11 \times 10^{-3}$ mm^2/s (21). However it was slightly lower than the value previously reported by Kilickesmez et al. (10) who found the mean ADC value of 9 Pca patients was $1.06 \pm 0.17 \times 10^{-3}$ mm^2/s. It was also lower than the value of Tamada et al. (13) who reported a mean ADC value of $1.02 \pm 0.25 \times 10^{-3}$ mm^2/s. Conversely it was slightly higher than the value previously reported by Abdel-Maboud et al. (22) who found that mean ADC value of 31 cases of PCa was $0.737 \pm 0.154 \times 10^{-3}$ mm^2/s.

Kılıçkesmez et al. (10) previously stated that the variation in the reported ADC values of normal PZ, CG of the prostate gland, and PCa may be related to the strength of the diffusion gradient (300–1000 s/mm^2), and the magnetic field (1.5 or 3 T) used.

There was a significant difference between the ADC measurement of benign and malignant prostatic lesions with a ρ value <0.05. This was in agreement with the previous reports of Yagci et al. (23), Tamada et al. (13) and Kilickesmez et al. (10). This was in concordance with the results of Ren and his colleagues (2) who have found a statistically significant difference in the mean ADC values for the normal CG, PZ, prostate cyst, BPH nodules and PCa foci with ρ values <0.05.

Kim and his colleagues (24) previously reported that even with high b values, the overlap of the ADC values between cancer and benign prostatic tissue limits the accuracy of DWI in cancer detection, particularly in the transitional zone tissue, due to its lower ADC compared to the peripheral zone tissue. Akgun et al. (25) have stated that with any b value, the assessment of the diffusion restriction should only be performed as a part of routine multiparametric radiologic evaluation of the prostate gland. In addition, in lesions with small diameters, they suggest evaluating the diffusion restriction by

a visual assessment of ADC maps instead of measuring ADC values, which can be challenging. (25).

In the present study, although the mean ADC values of prostate cancer DWI were significantly lower than those of benign prostatic tissues and BPH, considerable overlaps were found between the cancer and benign prostatic tissues. Therefore, we suppose that the use of ADC values alone could result in the misdiagnosis of prostate cancer.

We compared the performance of T2 weighted MRI alone versus T2 combined with DWI in localization of PCa. We have found that the use of combined T2WI and DWI was able to localize PCa better than T2 WI alone.

The accuracy, sensitivity and specificity for combined T2 with DWI were 90%, 85% and 95% respectively compared to 77.5%, 65% and 90% when using T2 alone. Our results were in concordance with those of the previous study of Yagci et al. (23) who have reported a better performance of T2 combined with DWI compared to T2 alone in prostate cancer localization, with an accuracy of 89% vs 76%, specificity of 92% vs 77% and sensitivity of 81% vs 71%. Haider et al. (7) have reported accuracy, sensitivity, and specificity of combined T2 and diffusion 83%, 81% and 91% compared with 77%, 54% and 84% when using T2 alone.

6. The study has few limitations

The use of pelvic phased array coil resulted in less SNR in the area of the prostate and poor image quality, however the use of high field strengths and higher b-values can improve lesion detection. In addition not all MRI findings compared with pathological results after prostatectomy, with some pathological results were based on TRUS-guided biopsy, and it should be noted that some TRUS-guided biopsies may give false negative results.

6.1. In conclusion

DWI appearance and ADC values can differentiate between PCa and BPH. For localization of PCa the combined use of T2 and DWI was better than using T2 alone. So, DWI with ADC measurement can be used as a complementary imaging method to conventional MRI in diagnosis of prostatic carcinoma and benign prostatic hyperplasia.

Conflict of interest

The authors declare no conflict of interests.

Acknowledgments

The authors would like to thank Mrs. Hala Mohamed in the Department of Radiology, Cairo University for the MRI scanning. The authors would also like to thank Dr. Mohammed Rafaat in the Department of Radiology, Cairo University and Dr. Tamer Moustafa in the Department of Radiology, National Cancer Institute for their assistance.

References

(1) Jemal A, Siegel R, Ward E, Murray T, Xu J, Smigal C, et al. Cancer statistics. Cancer J Clin 2006;56:106–30.

(2) Ren J, Yi Huan, He Wang, HaiTao Zhao, YaLi Ge, YingJuan Chang, et al. Diffusion-weighted imaging in normal prostate and differential diagnosis of prostate diseases. Abdom Imaging 2008; 33:724–8.

(3) Hoeks CMA, Barentsz JO, Hambrock T, Yakar D, Somford DM, Heijmink SWTPJ, Scheenen TWJ, Vos PC, Huisman HM, van Oort I, Witjes JA, Heerschap A, Fütterer JJ. Prostate cancer: multiparametric MR Imaging for Detection, Localization, and Staging. Radiology 2011;261:46–66.

(4) Nagel KN, Schouten MG, Hambrock T, et al. Differentiation of prostatitis and prostate cancer by using diffusion-weighted MR imaging and MR-guided biopsy at 3 T. Radiology 2013;267: 164–72.

(5) Sato C, Naganawa S, Nakamura T, Kumada H, Miura S, Takizawa O, et al. Differentiation of noncancerous tissue and cancer lesions by apparent diffusion coefficient values in transition and peripheral zones of the prostate. J Magn Reson Imaging 2005;21:258–62.

(6) Desouza NM, reinsberg SA, Scurr ED, Brewster JM, Payne GS. Magnetic resonance imaging in prostate cancer: the value of apparent diffusion coefficients for identifying malignant nodules. Br J Radiol 2007;80:90–5.

(7) Haider MA, van der Kwast TH, Tanguay J, Evans AJ, Hashmi AT, Lockwood G, et al. Combined T2-Weighted and Diffusion-Weighted MRI for Localization of Prostate Cancer. Am J Roentgenol 2007;189(2):323–8.

(8) Tamada T, Sone T, Jo Y, et al. Apparent diffusion coefficient values in peripheral and transition zones of the prostate: comparison between normal and malignant prostatic tissues and correlation with histologic grade. J Magn Reson Imaging 2008;28(3):720–6.

(9) Petraliaa G, Thoeny HC. DW-MRI of the urogenital tract: applications in oncology. Cancer Imaging 2010;10(1A):S112–23.

(10) Kılıçkesmez Z, Cimilli T, İnci E, Kayhan A, Bayramoğlu S, Taşdelen N, et al. Diffusion-weighted MRI of urinary bladder and prostate cancers. Diagn Interv Radiol 2009;15:104–10.

(11) Somford DM, Fütterer JJ, Hambrock T, Barentsz JO. Diffusion and perfusion MR imaging of the prostate. Magn Reson Imaging Clin N Am 2008;16:685–95.

(12) Kim CK, Park BK, Lee HM, Kwon GY. Value of diffusion weighted imaging for the prediction of prostate cancer location at 3T using a phased-array coil: preliminary results. Invest Radiol 2007;42:8427.

(13) Tamada T, Sone T, Toshimitsu S, et al. Age-related and zonal anatomical changes of apparent diffusion coefficient values in normal human prostatic tissues. J Magn Reson Imaging 2008;27: 552–6.

(14) Anderson AW, Xie J, Pizzonia J, Bronen RA, Spencer DD, Gore JC. Effects of cell volume fraction changes on apparent diffusion in human cells. Magn Reson Imaging 2000;18:689–95.

(15) Song SK, Qu Z, Garabedian EM, Gordon JI, Milbrandt J, Ackerman JJ. Improved magnetic resonance imaging detection of prostate cancer in a transgenic mouse model. Cancer Res 2002;62: 1555–8.

(16) Boonsirikamchai P, Choi S, Frank SJ, Ma J, Elsayes K, Kaur H, et al. MR imaging of prostate cancer in radiation oncology: What radiologists need to know. RadioGraphics 2013;33:741–61.

(17) Yoshimitsu K, Kiyoshima K, Irie H, Tajima, Asayama Y, et al. Usefulness of apparent diffusion coefficient map in diagnosing prostate carcinoma: correlation with stepwise histopathology. J Magn Reson Imaging 2008;27:132–9.

(18) Hosseinzadeh K, Schwarz SD. Endorectal diffusion-weighted imaging in prostate cancer to differentiate malignant and benign peripheral zone tissue. J Magn Reson Imaging 2004;20(4):654–61.

(19) Liu X, Peng W, Liangping Zhou L, Wang H. Biexponential apparent diffusion coefficients values in the prostate: comparison among normal tissue, prostate cancer, benign prostatic hyperplasia and prostatitis. Korean J Radiol 2013;14(2):222–32.

(20) Chagas MA, Babinski MA, Costa WS, Sampaio FJ. Stromal and acinar components of the transition zone in normal and hyperplastic human prostate. BJU Int 2002;89:699–702.
(21) Tanimoto A, Nakashima J, Kohno H, Shinmoto H, Kuribayashi S. Prostate cancer screening: the clinical value of diffusion-weighted imaging and dynamic MR imaging in combination with T2-weighted imaging. J Magn Reson Imaging 2007;25:146–52.
(22) Abdelmaboud NM, Elsaid HH, Aboubeih EA. The role of diffusion-weighted MRI in evaluation of prostate cancer. EJRNM 2014(45):231–6.
(23) Yağcı AB, Özarı N, Aybek Z, Düzcan E. The value of diffusion-weighted MRI for prostate cancer detection and localization. Diagn Interv Radiol 2011;17:130–4.
(24) Kim JK, Jang YJ, Cho G. Multidisciplinary functional MR imaging for prostate cancer. Korean J Radiol 2009;10:535–51.
(25) Akgun V, Karaman B, Battal B, Sari S. RE: diffusion-weighted imaging of prostate cancer: How can we use it accurately? Korean J Radiol 2013;14(5):865–7.